

Observation of Barnett fields in solids by nuclear magnetic resonance

To cite this article: Hiroyuki Chudo *et al* 2014 *Appl. Phys. Express* **7** 063004

View the [article online](#) for updates and enhancements.

You may also like

- [Applications of nanomagnets as dynamical systems: II](#)
Bivas Rana, Amrit Kumar Mondal, Supriyo Bandyopadhyay et al.
- [Reply to "Comment on 'Observation of Barnett fields in solids by nuclear magnetic resonance'" \[Appl. Phys. Express 7, 063004 \(2014\)\]](#)
Hiroyuki Chudo, Mamoru Matsuo, Kazuya Harii et al.
- [Rock physics model-based prediction of shear wave velocity in the Barnett Shale formation](#)
Zhiqi Guo and Xiang-Yang Li

Observation of Barnett fields in solids by nuclear magnetic resonance

Hiroyuki Chudo^{1,3}, Masao Ono^{1,3}, Kazuya Harii^{1,3}, Mamoru Matsuo^{1,3}, Jun'ichi Ieda^{1,3}, Rie Haruki^{1,3}, Satoru Okayasu^{1,3}, Sadamichi Maekawa^{1,3}, Hiroshi Yasuoka¹, and Eiji Saitoh^{1,2,3,4}

¹Advanced Science Research Center, Japan Atomic Energy Agency, Tokai, Ibaraki 319-1195, Japan

²Institute for Materials Research, Tohoku University, Sendai 980-8577, Japan

³CREST, Japan Science and Technology Agency, Chiyoda, Tokyo 102-0075, Japan

⁴WPI-Advanced Institute for Materials Research, Tohoku University, Sendai 980-8577, Japan

Received April 4, 2014; accepted April 30, 2014; published online May 21, 2014

A magnetic field is predicted to emerge on a particle in a rotating material body even if the body is electrically neutral. This emergent field is called a Barnett field. We show that nuclear magnetic resonance (NMR) enables direct measurement of the Barnett field in solids. We rotated both a sample and an NMR coil synchronously at high speed and found an NMR shift whose sign reflects that of the nuclear magnetic moments. This result provides direct evidence of the Barnett field. The use of NMR for Barnett field measurement enables the unknown signs of nuclear magnetic moments in solids to be determined. © 2014 The Japan Society of Applied Physics

There are two physical mechanisms in which magnetism and mechanical rotation are combined: the Einstein–de Haas (EdH) effect^{1,2)} and the Barnett effect.^{3,4)} The former refers to the phenomenon in which, when a material body is magnetized by applying a magnetic field, it starts rotating as a consequence of conservation of the angular momentum of the magnetization and the body. The EdH effect has shown promise in application to nanomechanics and spintronics.^{5–8)} The reciprocal of the EdH effect, the Barnett effect, posits that an electrically neutral body is magnetized when it is rotated. This magnetization was observed and discussed phenomenologically by introducing an emergent magnetic field (Fig. 1).^{3,4)} Then the microscopic mechanism of this field was rigorously formulated in terms of quantum mechanics and general relativity.^{9–11)} According to these theories, the emergent field, which originates from the coupling between an electron spin and mechanical rotation, is the essence of the magnetization related to the Barnett effect.^{10,11)} This emergent field is hereafter called the Barnett field.

The Barnett field acting on a spin emerges by coordinate transformation from the laboratory frame to the rotating one:^{10–12)}

$$\begin{aligned} H &= UH_0U^\dagger - i\hbar U \frac{\partial U^\dagger}{\partial t} = H_0 - \mathbf{J} \cdot \boldsymbol{\Omega} \\ &= \frac{\mathbf{p}^2}{2m} - (\mathbf{r} \times \mathbf{p}) \cdot \boldsymbol{\Omega} + \mathbf{I} \cdot \gamma(\mathbf{B} + \mathbf{B}_\Omega), \end{aligned} \quad (1)$$

where $H_0 = \mathbf{p}^2/2m - \mathbf{I} \cdot \gamma\mathbf{B}$ is the Hamiltonian of a spin in the laboratory frame, m is the particle's mass, \mathbf{I} is the total spin, and \mathbf{B} is the external magnetic field. Further, $\gamma = gq/2m$ is the gyromagnetic ratio, where g is the g -factor, and q is the charge. The unitary transformation is given by $U = \exp[i\mathbf{J} \cdot \boldsymbol{\Omega}t/\hbar]$, where $\mathbf{J} = \mathbf{r} \times \mathbf{p} + \mathbf{I}$ is the generator of the rotation, and $\boldsymbol{\Omega}$ is the angular velocity. The last term in Eq. (1) indicates that the magnetic field \mathbf{B} is modified by the Barnett field:

$$\mathbf{B}_\Omega = \frac{2m}{gq} \boldsymbol{\Omega}. \quad (2)$$

The Barnett field is proportional to the particle's rest mass. Because atomic nuclei are much more massive than electrons, relatively large Barnett fields are expected to act on nuclei. In addition, the Barnett field acting on the nucleus depends on the nuclear g -factor. Thus, a difference in the g -factor causes

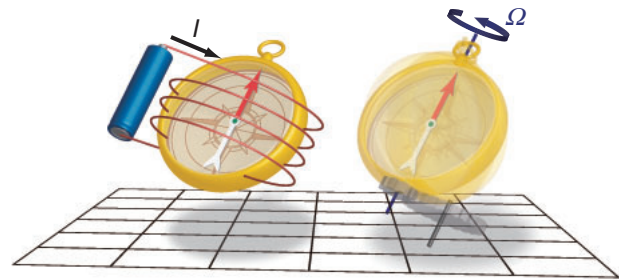


Fig. 1. Concept of a Barnett field. Magnetic fields are conventionally generated by establishing an electric current I in wires (left panel). The Barnett field is the magnetic field generated by rotating an object at the angular velocity $\boldsymbol{\Omega}$ (right panel). This field is directed along the axis of rotation and appears even in electrically neutral objects.

the magnitude of the Barnett field to vary even in the same material. In this report, we describe the direct observation of Barnett fields as a resonance shift in the nuclear magnetic resonance (NMR) under sample rotation.

The phenomenon of NMR proceeds by energy absorption and emission of an oscillating radio frequency (RF) field, $\mathbf{B}_x(\omega)$, applied perpendicular to the direction of a static magnetic field, \mathbf{B}_0 . The condition for NMR is the well-known formula

$$\omega_n = 2\pi f_n = |\gamma_n \mathbf{B}_n|, \quad (3)$$

where f_n , γ_n , and \mathbf{B}_n are the frequency of the RF field, the nuclear gyromagnetic ratio, and the local static field acting on a nucleus, respectively.¹³⁾ Neglecting small contributions from surrounding electron clouds, the local static field acting on the nucleus is the sum of an external field and the Barnett field; that is, $\mathbf{B}_n = \mathbf{B}_0 + \mathbf{B}_\Omega$. Thus, the value of \mathbf{B}_Ω can be measured precisely as a resonance shift by measuring either the frequency for resonance under a constant field \mathbf{B}_0 or the field for resonance under a constant frequency.¹⁴⁾ To measure \mathbf{B}_Ω using NMR, however, the sample and the NMR detection coil should be in the same frame of reference.¹⁵⁾ Therefore, by further extending the coil-spinning technique,¹⁶⁾ both the sample and the tuning circuit for NMR in this experiment were rotated rapidly with respect to the direction of \mathbf{B}_0 at exactly the same angular velocity.

In Fig. 2(a), we show a schematic illustration of the experimental assembly used in this study. The assembly consists of two components: the stationary coil placed along \mathbf{B}_0 and

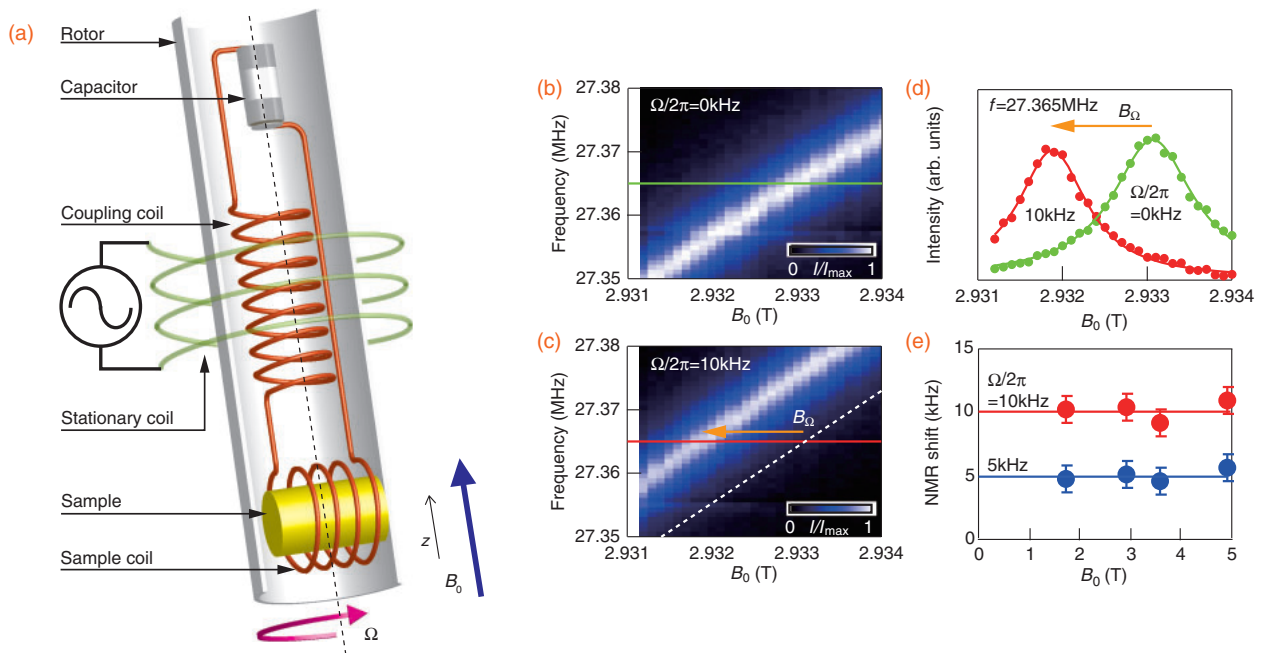


Fig. 2. Illustration of experimental assembly and evidence for Barnett field acting on ^{115}In nuclei. (a) Schematic of rotor and tuning unit for measurements. Inside the rotor, the coupling coil, sample coil, and capacitor form the tuning circuit tuned at the measurement frequency. The stationary and coupling coils are coupled via mutual induction. The axes of the stationary coil, coupling coil, and rotation, and the direction of the external magnetic field are parallel to the z -axis. The axis of the sample coil is perpendicular to the z -axis. (b, c) White-scale image plots of the ^{115}In NMR intensity obtained using the FFT-NMR method without and with rotation, respectively, at $\Omega/2\pi = +10$ kHz and a measurement frequency of 27.365 MHz under various magnetic fields. White dotted line in (c) graphs the results based on Eq. (3) (see text). (d) ^{115}In NMR intensity spectra as functions of magnetic field at measured frequencies corresponding to green line in (b) and red line in (c). (e) External magnetic field B_0 dependence of the ^{115}In NMR shifts caused by sample rotation at $\Omega/2\pi = +5$ and $+10$ kHz. The origin of the longitudinal axis is defined as the peak position of the NMR spectrum obtained at $\Omega = 0$.

connected to an NMR spectrometer, and a high-speed rotor consisting of a cylindrical capsule in which a specially arranged tuning circuit is installed. This circuit is composed of two small coils placed perpendicularly and connected in series, and a small capacitor. One of the two coils is arranged parallel to the stationary coil to establish coupling by mutual inductance between the tuning circuit and the stationary coil. We call this the coupling coil. The other coil, the sample coil, holds a sample inside. The RF field in the coupling coil is transmitted to the sample coil and generates the oscillating RF field $\mathbf{B}_x(\omega)$ to induce an NMR signal. Under this configuration, the sample coil rotates at exactly the same angular velocity as the sample, thereby fulfilling the conditions for observing \mathbf{B}_Ω . The rotor is placed inside the stationary coil, and during measurements, it is rotated up to $|\Omega/2\pi| = 10$ kHz. For $\Omega \parallel \mathbf{B}_0$, the sign of Ω is defined as positive.

Powdered samples of LiF, NaCl, InP, SnO_2 , and Si were used for the NMR measurements. To obtain NMR signals with high S/N ratios, ^{119}Sn and ^{29}Si were enriched. Although ^{23}Na and ^7Li , with $I = 3/2$, and ^{115}In , with $I = 9/2$, have quadrupole moments, no quadrupole splitting was observed in the NMR spectra because of the local cubic symmetry at the nuclear sites in these compounds. SnO_2 has a tetragonal rutile crystalline structure, but ^{119}Sn does not have a quadrupole moment. For signal acquisition, we employed a standard single $\pi/2$ pulse technique. The NMR spectra were obtained by fast Fourier transformation (FFT) of the free induction decay signals. All the measurements were performed at room temperature.

Our first step in observing the Barnett field was to record the ^{115}In NMR shifts in the nonmetallic, nonmagnetic com-

pound InP. To check the NMR detection using the tuning circuit described above, we measured the ^{115}In NMR spectra as a function of the externally applied field \mathbf{B}_0 without sample rotation. The results are shown in Fig. 2(b), using a white scale for the spectrum profile. From a linear fit of the NMR center frequency to Eq. (3) with $\mathbf{B}_\Omega = 0$, we found γ_n for ^{115}In in InP to be $|^{115}\gamma_n|/2\pi = 9.330$ MHz/T, which agrees well with the reported value of 9.3858 MHz/T.¹⁷⁾ This fact indicates that the system was working properly to observe Barnett fields.

We then rotated the rotor while monitoring the NMR signal. In Fig. 2(c), we show the external field dependence of the NMR center frequency at an angular velocity of $\Omega/2\pi = +10$ kHz parallel to the external field. The NMR center frequencies increase under rotation; that is, the nuclei feel an extra field in addition to the external field. If there is no change in $^{115}\gamma_n$ with mechanical rotation, the data can be fitted to $f_n = |^{115}\gamma_n(\mathbf{B}_0 + \mathbf{B}_\Omega)|/2\pi$. The Barnett field \mathbf{B}_Ω is estimated to be $+1.1 \pm 0.10$ mT, which is represented by the orange arrows in Figs. 2(c) and 2(d). This is the first direct measurement of the Barnett field. We have confirmed that the Barnett field acting on the nuclei is independent of the external magnetic field [Fig. 2(e)], which implies that the Barnett field emerges because of rotation even under zero external magnetic field.

In Fig. 3(a), we plot the ^{115}In NMR spectra at various values of the angular velocity Ω . The external magnetic field is fixed at $B_0 = 2.75$ T. Clearly, the NMR center frequency increases linearly with Ω as given by Eqs. (2) and (3). Furthermore, by reversing the rotation direction ($\Omega < 0$), the direction of the NMR shift is also reversed [compare red and

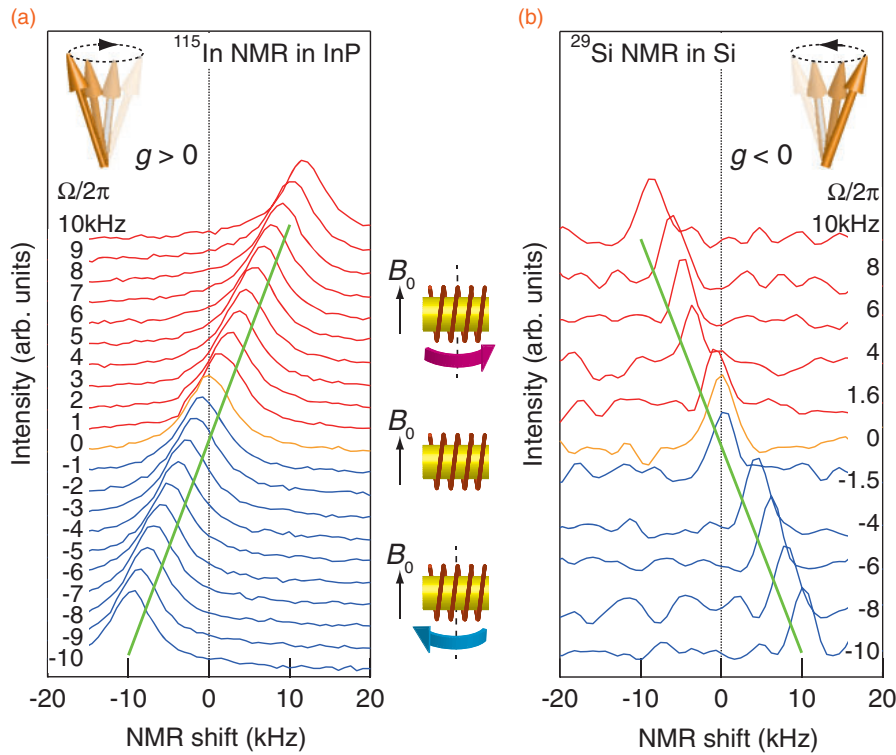


Fig. 3. NMR spectra for positive and negative g -factors. Spectra for (a) ^{115}In and (b) ^{29}Si NMR obtained at various angular velocities. The origin of the transverse axis is defined as the peak position of the NMR spectrum obtained at $\Omega = 0$ (orange curve). The green lines are guides to the eye.

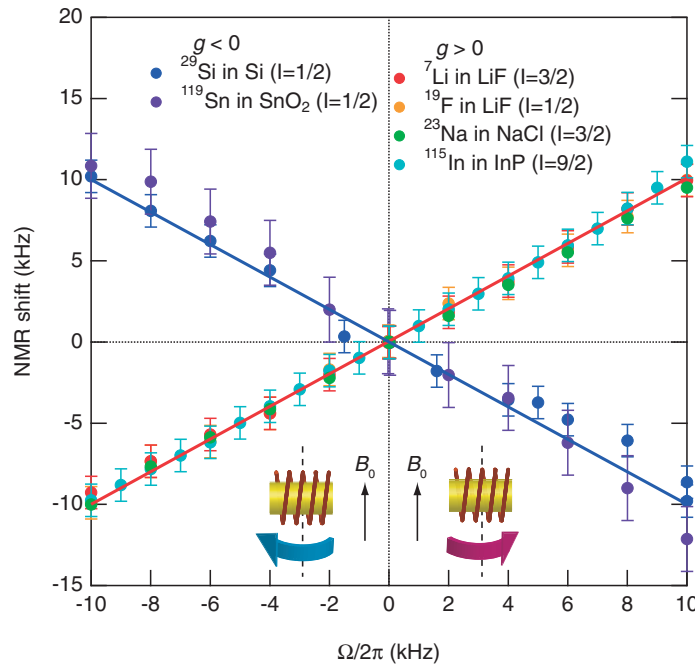


Fig. 4. Universal behavior of NMR shifts as a function of the angular velocity Ω . ^7Li in LiF (red dots), ^{19}F in LiF (orange dots), ^{23}Na in NaCl (green dots), and ^{115}In in InP (light-blue dots) have positive g -factors. ^{29}Si in Si (blue dots) and ^{119}Sn in SnO_2 (purple dots) have negative g -factors. Vertical axis represents NMR shifts; its origin is determined by the center frequency at $\Omega = 0$ for each sample. Red and blue lines are theoretical predictions based on Eqs. (2) and (3) (see text).

blue curves in Fig. 3(a)]; thus, the sign of \mathbf{B}_Ω is reversed. The Barnett field acting on each nucleus is proportional to the angular velocity, including its sign.

The sign of the g -factor of ^{115}In is known to be positive;¹⁷⁾ that is, the nuclear magnetic moment is parallel to its angular momentum. Next, we measured the shifts for nuclei with

negative g -factors. Equation (2) predicts that the Barnett fields reveal the sign of the g -factors. From the NMR spectra for ^{29}Si , which has a negative g -factor,¹⁷⁾ the direction of the NMR shift [Fig. 3(b)] is clearly opposite to that for ^{115}In , indicating that the emergent Barnett field is opposite in direction to that for ^{115}In . We collected the NMR shifts for

various nuclei as a function of Ω (Fig. 4). In each sample, the NMR shift exhibits linear dependence on Ω . The g -factors for ${}^7\text{Li}$, ${}^{19}\text{F}$, ${}^{23}\text{Na}$, and ${}^{115}\text{In}$ are known to be positive, whereas those for ${}^{29}\text{Si}$ and ${}^{119}\text{Sn}$ are negative.¹⁷⁾ All the nuclei with positive g -factors display positive slopes (red line in Fig. 4), whereas all the nuclei with negative g -factors display a negative slope (blue line), which is consistent with Eq. (2).

We emphasize that the proposed technique realizes a new way of determining the sign of the g -factor in solids. In some nuclei, the sign is still difficult to determine.^{18–20)} The scope of solid-state science is currently expanding to involve heavy elements. The recent discovery of NMR signals from ${}^{239}\text{Pu}$ was highly newsworthy,¹⁸⁾ and NMR in many nuclei remains to be discovered. For such nuclei, only minute amounts of solid are available for sampling; thus, the proposed technique may provide an exclusive method of resolving this issue because coil spinning is a unique method that enables NMR measurement of minute samples.¹⁶⁾

In the above discussion, we assumed that, for Eq. (2), the renormalization of the rotation effect on nuclear spins is absent in the zeroth-order approximation. With this assumption, Eq. (2) explains the experimental results within the resolution of these measurements, as demonstrated by Fig. 4. The next step is to introduce the renormalization for higher-order coupling.²¹⁾ This effect modifies the nuclear g -factors; namely, the slope deviates from unity in Fig. 4. When considering these modifications, it is helpful to refer to EdH studies of electronic systems.^{22–24)} In electronic systems, the spectroscopic g -factors are generally different from the gyroscopic g -factors. This difference arises from the fact that the gyroscopic effect combines the total angular momentum with rotation, whereas the Zeeman effect combines the total magnetic moment with a magnetic field.¹⁴⁾ This difference enables estimation of the orbital angular momentum of electrons in solids. In contrast, modification of the nuclear g -factors reveals richer physics. The nucleus contains protons, neutrons, and mesons. All of them contribute to the orbital angular momentum, but only some can contribute to the orbital magnetic moments because neutrons are electrically neutral.^{25–27)} Therefore, the Barnett field will provide a way to investigate such features of the nuclei, although the experimental resolution is currently not sufficient to estimate this deviation. Improving the field resolution is thus certainly worthwhile, as is applying the proposed technique to a wide range of issues.

In conclusion, we developed a new coil-spinning NMR method of detecting the Barnett field. The Barnett field is observed as an NMR shift proportional to the rotation speed. The sign of the Barnett field depends on both the sign of the nuclear magnetic moment and the rotation direction against the external magnetic field. These features can be

used to determine the unknown sign of the nuclear magnetic moment. Our findings provide direct evidence of the coupling between the nuclear magnetic moment and mechanical rotation, and will produce new technology in which mechanical motion manipulates the nuclear spin angular momentum as well as the electron spin angular momentum.

Acknowledgments The authors thank A. Nakamura, S. Nagamiya, K. Imai, and T. Maruyama for valuable discussions. This work was financially supported by a Grant-in-Aid for Scientific Research C (22540354), the Sumitomo Foundation, and Fundamental Research Grants from CREST-JST “Creation of Nanosystems with Novel Functions through Process Integration.”

- 1) O. W. Richardson, *Phys. Rev.* **26**, 248 (1908).
- 2) A. Einstein and W. J. de Haas, *Verh. Dtsch. Phys. Ges.* **17**, 152 (1915) [in German].
- 3) S. J. Barnett, *Phys. Rev.* **6**, 239 (1915).
- 4) S. J. Barnett, *Rev. Mod. Phys.* **7**, 129 (1935).
- 5) T. W. Wallis, J. Moreland, and P. Kabos, *Appl. Phys. Lett.* **89**, 122502 (2006).
- 6) R. Jaafar, E. M. Chudnovsky, and D. A. Garanin, *Phys. Rev. B* **79**, 104410 (2009).
- 7) G. Zolfagharkhani, A. Gaidarzhly, P. Degiovanni, S. Kettemann, P. Fulde, and P. Mohanty, *Nat. Nanotechnol.* **3**, 720 (2008).
- 8) K. F. Woodman, P. W. Franks, and M. D. Richards, *J. Navig.* **40**, 366 (1987).
- 9) F. W. Hehl and W.-T. Ni, *Phys. Rev. D* **42**, 2045 (1990).
- 10) M. Matsuo, J. Ieda, and S. Maekawa, *Phys. Rev. B* **87**, 115301 (2013).
- 11) J. Fröhlich and U. M. Studer, *Rev. Mod. Phys.* **65**, 733 (1993).
- 12) L. D. Landau and E. M. Lifshitz, *The Classical Theory of Fields* (Elsevier, Amsterdam, 2010) 4th ed., Chap. 5.
- 13) A. Abragam, *The Principles of Nuclear Magnetism* (Oxford University Press, Oxford, U.K., 1961) 4th ed., Chap. 5.
- 14) S. P. Heims and E. T. Jaynes, *Rev. Mod. Phys.* **34**, 143 (1962).
- 15) In the present system, the number of rotation degrees of freedom is two: the relative rotation and the absolute mean rotation. Accordingly, there are two independent rotation-induced mechanisms; the Barnett and the Doppler effects. The Barnett effect is governed by the absolute rotation speed measured from the laboratory frame of reference. In contrast, the Doppler effect is governed by the relative angular velocity between the coil and the sample, and thus is easily eliminated by setting the relative velocity zero. Therefore, to observe the Barnett effect, the sample and the coil must be in the same frame of reference.
- 16) D. Sakellariou, G. Le Goff, and J.-F. Jacquinot, *Nature* **447**, 694 (2007).
- 17) N. J. Stone, *At. Data Nucl. Data Tables* **90**, 75 (2005).
- 18) H. Yasuoka, G. Koutroulakis, H. Chudo, S. Richmond, D. K. Veirs, A. I. Smith, E. D. Bauer, J. D. Thompson, G. D. Jarvinen, and D. L. Clark, *Science* **336**, 901 (2012).
- 19) J. Faust, R. Marrus, and W. A. Nierenberg, *Phys. Lett.* **16**, 71 (1965).
- 20) J. O. Rasmussen and L. W. Chiao, *Proc. Int. Conf. Nuclear Structure*, 1960, p. 646.
- 21) H. Feshbach, *Theoretical Nuclear Physics: Nuclear Reactions* (Wiley, New York, 1991).
- 22) C. Kittel, *Phys. Rev.* **76**, 743 (1949).
- 23) J. H. Van Vleck, *Phys. Rev.* **78**, 266 (1950).
- 24) G. G. Scott, *Phys. Rev.* **82**, 542 (1951).
- 25) J. M. Blatt and V. F. Weisskopf, *Theoretical Nuclear Physics* (Dover, New York, 1979) Chap. 2.
- 26) Y. Futami, J. Fujita, and H. Ohtsubo, *Prog. Theor. Phys. Suppl.* **60**, 83 (1976).
- 27) H. Hyuga, A. Arima, and K. Shimizu, *Nucl. Phys. A* **336**, 363 (1980).